Joint Inversion of Geophysical Data for Site Characterization and Restoration Monitoring

FY97 Annual Progress Report for EMSP
Project #55411, TTP No. SF2-7-SP-22

P. A. Berge, J. G. Berryman, B. P. Bonner, J. J. Roberts, D. Wildenschild
Lawrence Livermore National Laboratory
P O Box 808
Livermore, CA 94550

Introduction

The purpose of this project is to develop a computer code for joint inversion of seismic and electrical data, to improve underground imaging for site characterization and remediation monitoring. The computer code developed in this project will invert geophysical data to obtain direct estimates of porosity and saturation underground, rather than inverting for seismic velocity and electrical resistivity or other geophysical properties. This is intended to be a significant improvement in the state-of-the-art of underground imaging, since interpretation of data collected at a contaminated site would become much less subjective.

The schedule of this project is as follows: In the first year, investigators perform laboratory measurements of elastic and electrical properties of sand-clay mixtures containing various fluids. Investigators also develop methods of relating measurable geophysical properties to porosity and saturation by using rock physics theories, geostatistical, and empirical techniques together with available laboratory measurements. In the second year, investigators finish any necessary laboratory measurements and apply the methods developed in the first year to invert available borehole log data to predict measured properties of cores and sediments from a borehole. Investigators refine the inversion code in the third year and carry out a field experiment to collect seismic and electrical data. Investigators then use the inversion code to invert the field data to produce estimates of porosity and saturation in the field area where the data were collected.

This report describes progress made in the first year of this three-year project. For more information on work planned for the second and third years, and for additional technical details, see either the original proposal submitted to the EMSP program or see the world-wide web homepage that we have created for this project, at the URL "http://www-ep.es.llnl.gov/www-ep/esd/expgeoph/Berge/EMSP/".

Background

Effective in-situ remediation requires a knowledge of subsurface porosity, permeability, and fluid saturation. Only after the site has been characterized can the clean-up begin. Using geophysical techniques to image the subsurface is much cheaper and less invasive than drilling many sampling wells. Electrical methods have usually been used for environmental applications, but recent advances in high-resolution crosswell seismic methods (e.g., Harris et al., 1995) suggest that combined electrical and seismic techniques

could be a powerful tool for imaging the shallow subsurface.

Surface and borehole geophysical data have been used for a number of years for site characterization and clean-up monitoring (e.g., Ramirez et al., 1993, 1995; Wilt et al., 1995a,b) and monitoring steam-flooding in hydrocarbon reservoirs (e.g., Harris, 1988; Mathisen et al., 1995), but these data may only indirectly measure the site structure and fluid flow parameters that control the storage and movement of subsurface fluids. The current practice in geophysics is to interpret a single geophysical data set to obtain an image of a single geophysical parameter, such as seismic velocity or electrical resistivity. The geologic parameters of interest (i.e., the permeability, porosity, and fluid distribution) are usually estimated by overlaying a series of these geophysical images. Current estimation techniques are very subjective, and geologic parameters are not obtained directly. Current practices also do not exploit the complementary capabilities of seismic and electrical methods. Seismic methods are best for resolving subsurface structure and porosity (e.g., Lines et al., 1993; Mathisen et al., 1995), whereas electrical methods are preferred for identifying fluids, saturation, and permeability (e.g., Wilt et al., 1995a,b).

The goal of our project is to develop a code for joint inversion of seismic and electrical data. We will invert these data to obtain direct estimates of the porosity and saturation, rather than inverting for seismic velocity and electrical resistivity. Our method exploits the complementary nature of seismic and electrical measurements, and leads to an objective estimate of the geological and fluid flow parameters that are of most interest. This approach provides a dual benefit to environmental site assessment. First, it provides a powerful set of tools for jointly inverting geophysical data; and secondly, it provides a common platform for visualizing the results. No longer will it be necessary to overlay disparate images to look for "common anomalies". Instead of comparing multiple images of electrical conductivity and seismic velocity for site information, we will examine single images of porosity and saturation that are derived from the geophysical data.

The ultimate objective of this work is to use geophysical and well-test data to provide accurate information about porosity, saturation, and permeability between wells. In this three-year project, we use a multi-phase approach consisting of theoretical and numerical code development, laboratory investigations, testing on available laboratory and borehole geophysics data sets, and a controlled field experiment, to develop practical tools for joint

electrical and seismic data interpretation. This report describes progress made in the first year, including theoretical development of physical properties relationships and laboratory investigations of electrical and elastic properties of sand-clay mixtures.

Progress in FY97

Development of the joint inversion code requires developing algorithms relating geophysical data to porosity and saturation. Work done in the first year of this project provides the basis for developing and testing the inversion code on borehole and field data in the second and third years of the project. We are developing the necessary algorithms using a flexible approach that will allow us to assess the relative usefulness of geostatistical methods, empirical techniques commonly used in borehole geophysics interpretation (e.g., Archie, 1942; Wyllie et al., 1956, 1958; Waxman and Smits, 1968), and rock physics theories (see Berryman, 1995 for a review) that describe how elastic wave velocities and electrical conductivities depend on porosity and saturation in porous materials having different microgeometries. Much of the code for the theoretical analysis already exists in various forms (e.g., Cheng, 1978; Berge et al., 1992, 1993, 1995; Berryman, 1995; Berryman and Berge, 1996). Existing effective medium theory algorithms that were developed for use with consolidated materials at moderately high pressure conditions must be modified for application to the near surface environment. Empirical methods that were mainly developed for consolidated materials and oil industry applications may or may not be effective for environmental applications.

In order to test these different techniques, we have made an exhaustive search of the marine geophysics, civil engineering, soil mechanics, exploration geophysics, and environmental geophysics literature to find available information on rock properties measurements for unconsolidated sands and clays at low pressures (i.e. shallow depths). We have compiled a database containing elastic properties data for unconsolidated sediments that we will use to modify and test the necessary algorithms for relating elastic properties to porosity and saturation for dry and fully saturated sediments. A representative portion of this database is included as an appendix to this report.

Since limited information is available for unconsolidated sediments at low pressures appropriate for the near-surface, particularly for sediments containing clays, we have made our own laboratory measurements for unconsol-

idated sand-clay mixtures and are in the process of reducing and interpretting both elastic and electrical properties data. Our laboratory equipment allows us to measure porosities and permeabilities as well as geophysical properties. This provides the needed information for developing relationships between geophysical properties and the hydrogeologic parameters that are most useful for environmental applications. (We will complete our laboratory measurements in the second year, concurrently developing and testing the inversion algorithm.)

Diagrams of our measurement apparatus and some preliminary results are included in the the "Experimental Results" subsection later in this report. Our preliminary results suggest that microstructure controls the geophysical properties. Thus microstructure assumptions used in empirical or theoretical methods may be the determining factor for which methods are most useful for developing the algorithms that relate geophysical properties to porosity and saturation.

In addition to the work on geophysical properties data, we have made progress in developing rock physics theories for estimating rock and sediment properties for mixtures such as unconsolidated sands and clays that may be dry or fully saturated. This progress is described in the "Progress on Theories" subsection below.

Experimental Results

We have been conducting a series of electrical and elastic properties measurements on a limited number of sand-clay mixtures, using filtered, deionized water, tap water, and KC1 brines of a few different salinities for the pore fluids. Fluid conductivities were measured using an Omega water analyzer. Dry and fully saturated samples were used, to simplify the velocity measurements since partial saturation introduces a significant degree of complexity to the problem. We have been investigating the effects of different clays such as kaolinite, bentonite, and a natural clay-rich soil called Alligator clay. We have used various mixing techniques to construct the sand-clay samples, since the microgeometry is a critical factor affecting measured elastic and electrical properties.

Future work will include measurements on contaminated soils that we have obtained from two boreholes at an LLNL site, as well as characterizing our samples using x-ray computed tomography to obtain microstructural information such as estimates of water content and indications of clay degradation and interaction with DNAPL pore fluids.

Electrical Properties

For the electrical properties measurements, we have made complex resistivity measurements over a large range of frequencies so that we can analyze the contributions of different conduction mechanisms to the overall electrical properties of a given sample. Complex resistivity measurements are often useful in determining the role of specific conduction mechanisms such as clay surface conduction (e.g., Olhoeft, 1985; Olhoeft and King, 1991; Garrouch and Sharma, 1994). Non-linear phenomena may be produced in clay-bearing rocks and sediments by cation exchange, surface conduction, and clay-organic reactions (e.g., Olhoeft, 1985; Ramirez et al., 1993).

One of our component systems has a function generator to supply current at frequencies between 0.001 and 10^5 Hz, and uses an EGG lock-in amplifier. Additional impedance measuring systems available in the LLNL Experimental Geophysics laboratory extend the range of frequencies we can use for our measurements. These three other systems have frequency ranges of 100 to 10^5 Hz and 10 Hz to 1 MHz for two HP LCR meter systems, and 10^{-5} to 10^5 Hz for an EGG electrochemical impedance system. Figures 1 and 2 show a schematic diagram and a photograph of part of the apparatus used for electrical measurements.

We are still in the process of reducing and analyzing the electrical properties results. Figures 3 through 8 show examples of some preliminary results for the electrical properties measurements.

We are currently experimenting with other types of electrodes, to reduce some of the sources of measurement uncertainty. Previous measurements were made using platinum wires. We are experimenting with Ag wires that we are trying to react with NaCl or KC1 solution to form AgCl on the wire. This should eliminate some electrode polarization problems. We are making progress on sample porosity and permeability measurements for the electrical apparatus. Presently we are using separate equipment for elastic and electrical properties measurements instead of using a single apparatus, because of difficulties with the measurement techniques interfering with each other and causing large uncertainties in results. We are using samples that are matched as closely as possible for the sand-clay mixtures, with respect to saturation, porosity, clay type, flocculation of clays, etc. Elastic wave velocity measurements will be discussed below, after the figures showing electrical measurements.

Fig. 1

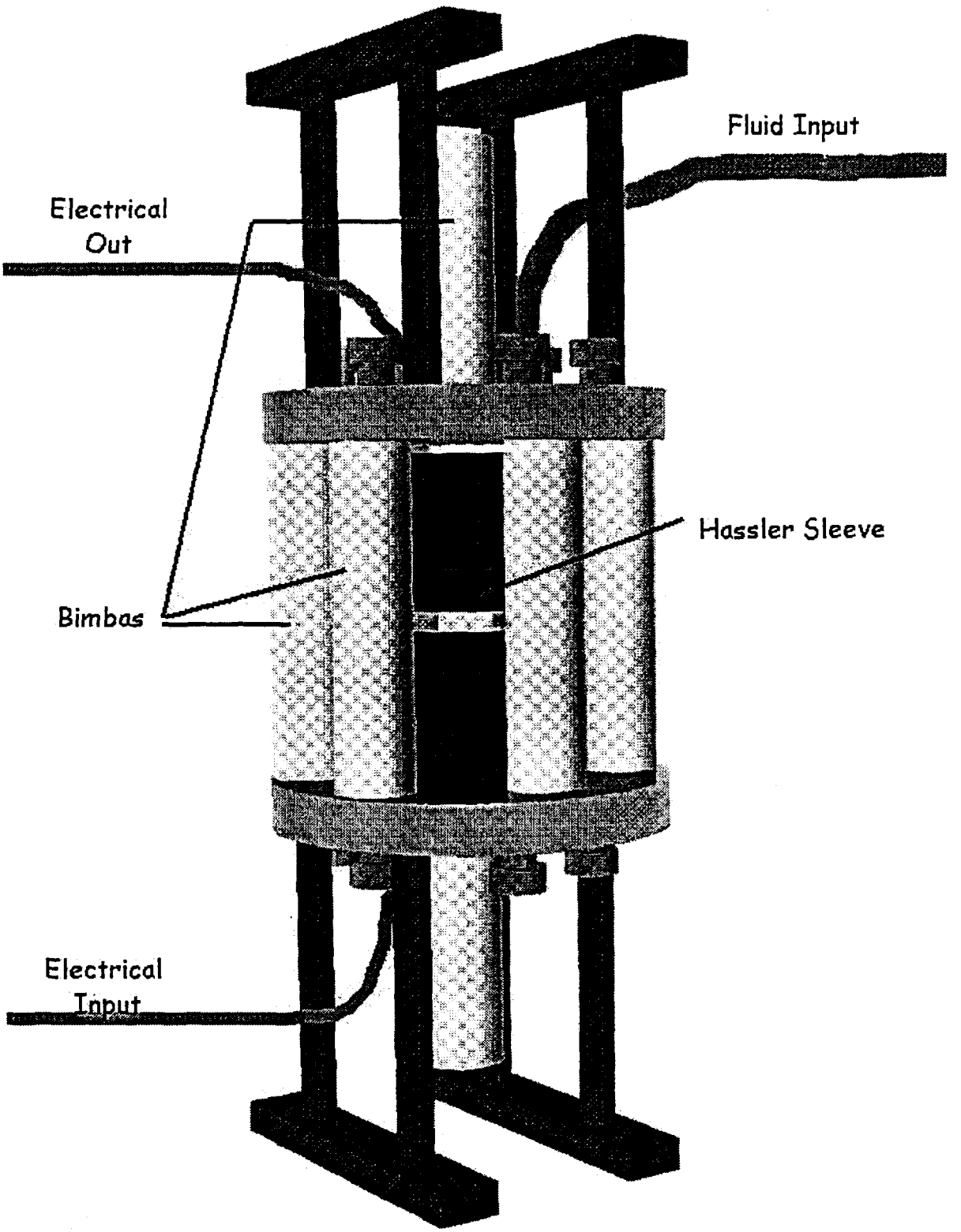
Fluid Input
Electrical Out
Hassler Sleeve
Bimbas
Electrical Input

Figure 1. 3D image of apparatus used to make electrical measurements on samples. The two-inch diameter sample is placed inside the Hassler sleeve, which applies confining pressure. Axial pressure is applied by the pneumatic cylinders around the perimeter and on the top and bottom. The fluid tube allows continuous input of various fluids. The electrical coaxial cables are used for electrical conductivity measurements.

Fig. 2

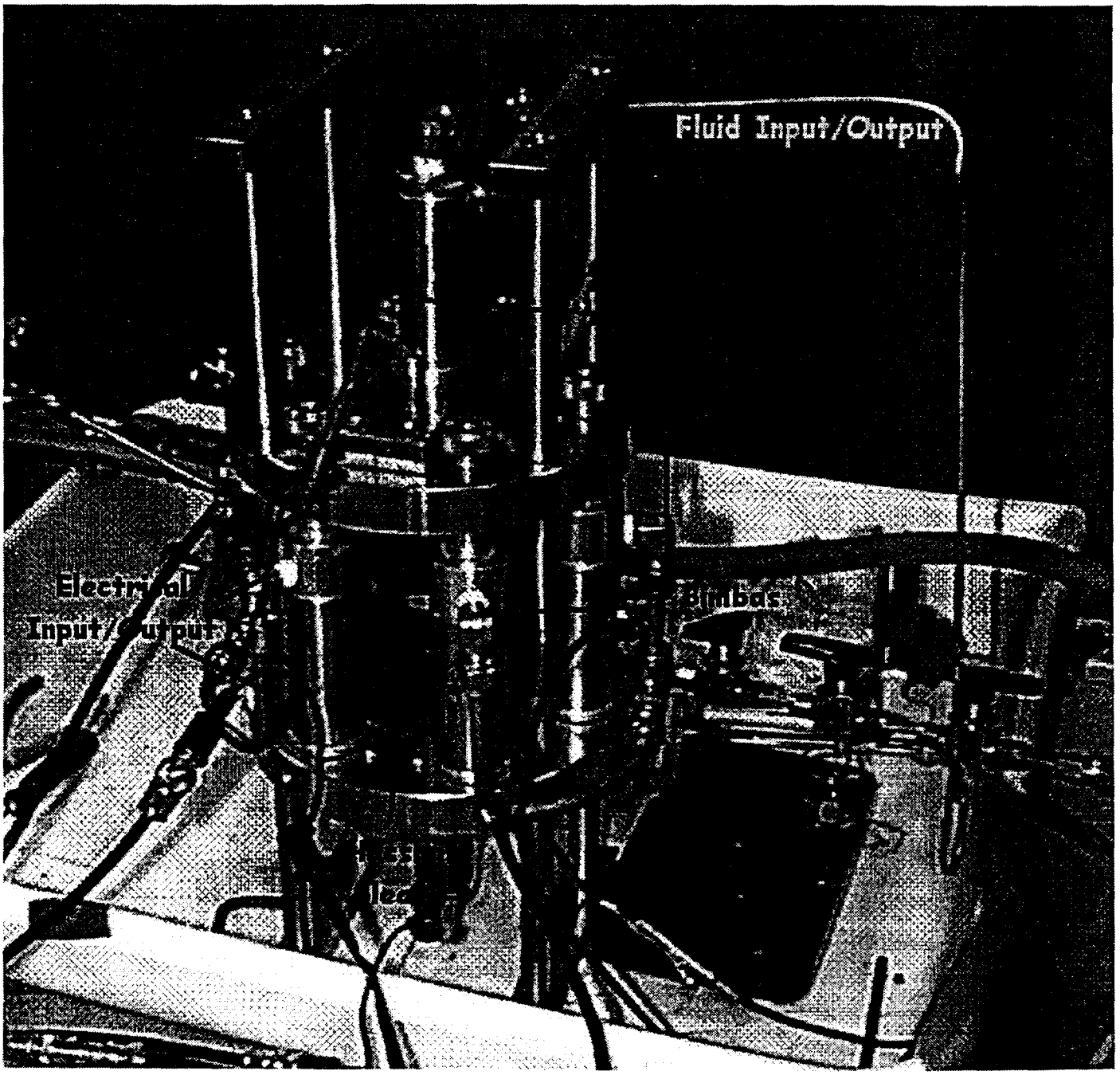

Figure 2. Photograph showing experimental setup for electrical measurements. The electrical measurements are made as a function of frequency between 1 MHz and 1 mHz for each sample. The four-electrode method is used. The metallic frits serve as the end electrodes and the wire loops work as the inner, voltage measuring electrodes. The use of different saturating fluids (with differing electrical conductivities) helps to determine the dominant conduction pathways through the sample.

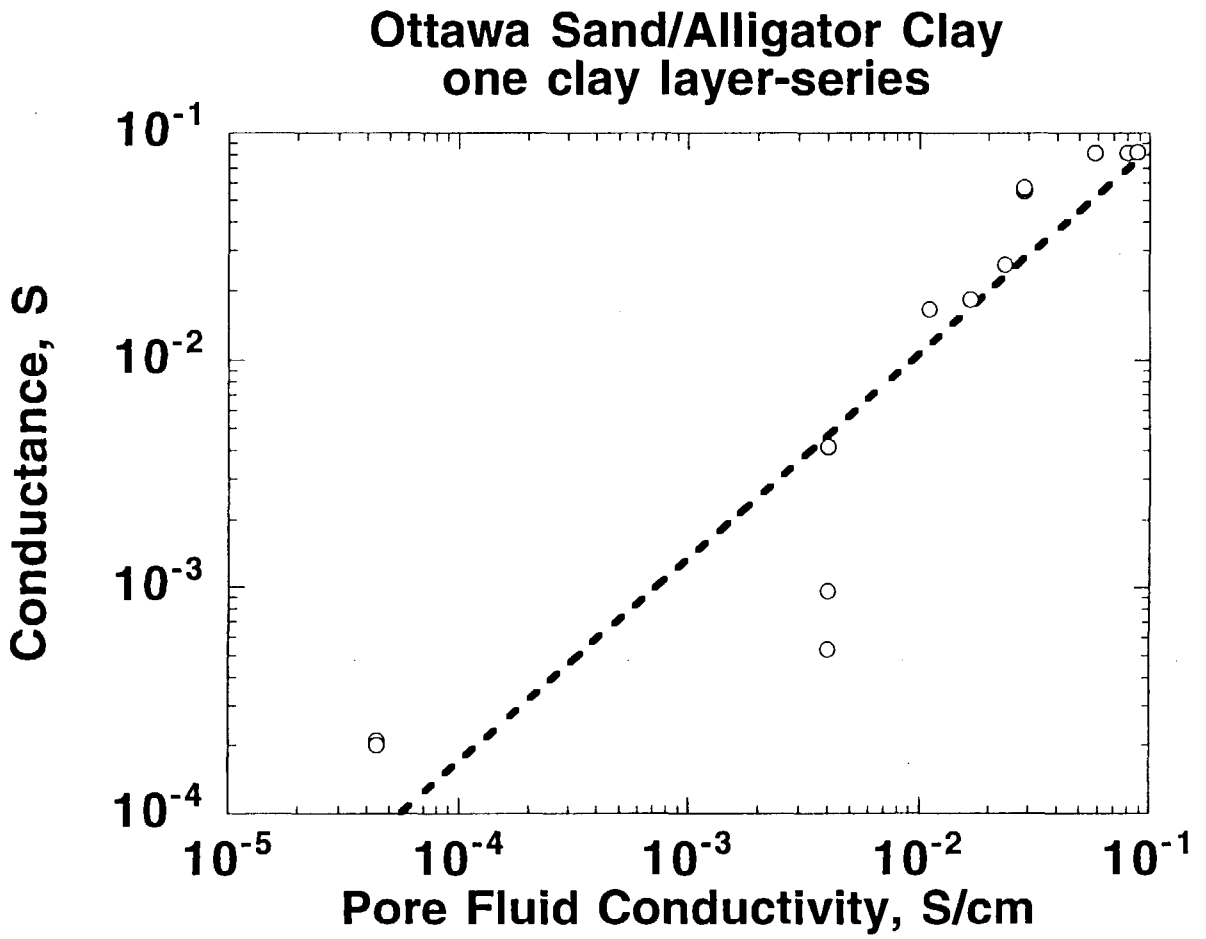
Ottawa Sand/Alligator Clay
one clay layer-series
Conductance, S
10^{-1}
10^{-2}
10^{-3}
10^{-4}
10^{-5}
10^{-4}
10^{-3}
10^{-2}
10^{-1}
Pore Fluid Conductivity, S/cm

Fig. 3

Figure 3. Sample conductance (l/resistance) vs. fluid conductivity (in siemens/cm) for a mixture of Ottawa sand and Alligator clay. There is one layer of clay. It is in series electrically; that is, the layer is parallel to the frit electrodes. The line is a fit that shows a roughly linear dependence on a log-log plot.

Conductance of Sand and Sand-Clay Mixtures

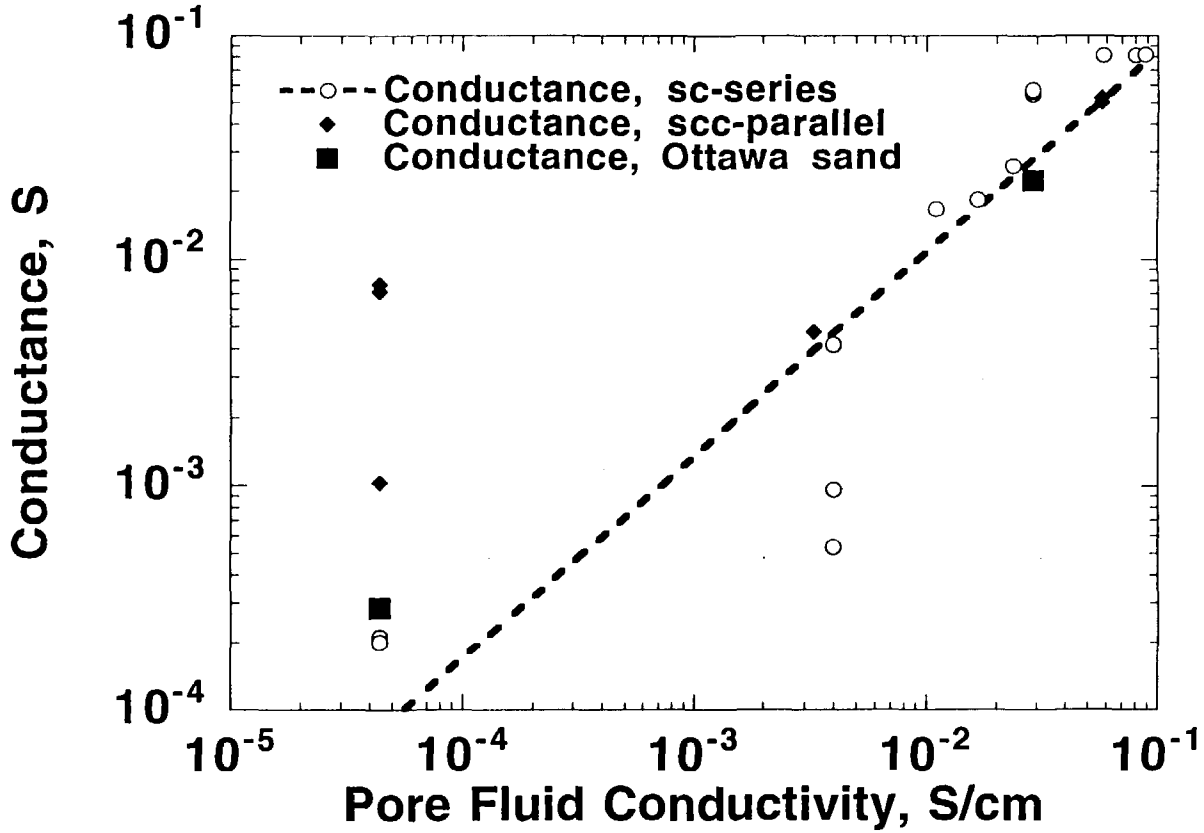

Fig. 4

Figure 4. Similar to Figure 3, with the addition of a few data points from other configurations. x-series is the same as Figure 3. scc-parallel is a clay layer that is in parallel electrically; that is, perpendicular to the electrodes. Ottawa sand is a strictly sand sample. The sand sample and series sample are essentially the same. The series clay layer has very little effect on conductivity. What is different is the parallel clay layer sample, which is more conductive at lower fluid conductivities. (More study should be done before any strong conclusions are drawn from this.)

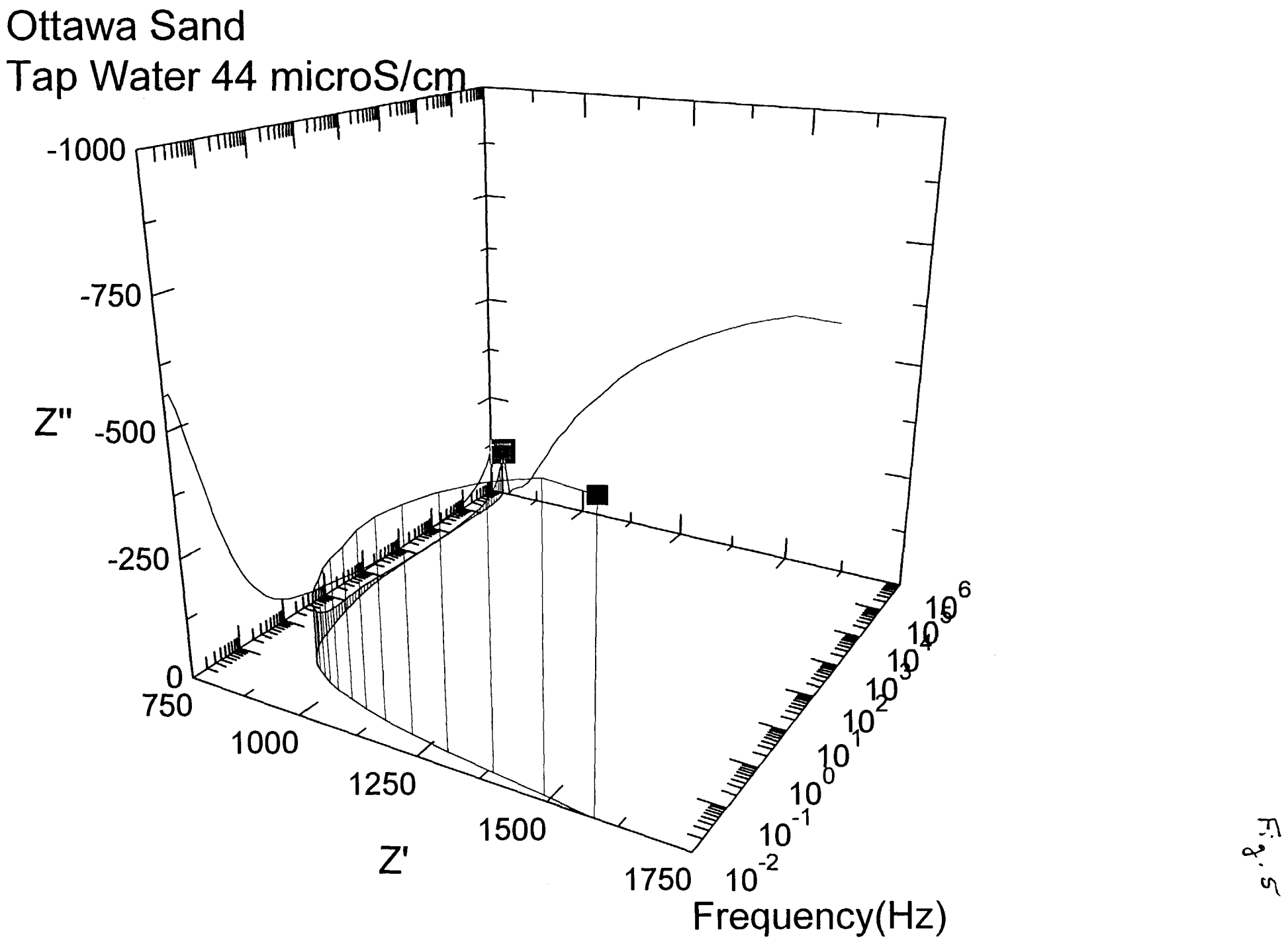
Ottawa Sand
Tap Water 44 microS/cm
-1000
-750
-500
-250
0
Z''
750
1000
1250
1500
1750
Z'
10^{-2}
10^{-1}
10^{0}
10^{1}
10^{2}
10^{3}
10^{4}
10^{5}
10^{6}
Frequency(Hz)

Fig. 5

Figure 5. This shows the frequency-dependent electrical properties of a sample of 100% Ottawa sand and tap water (44 μS/cm conductivity).

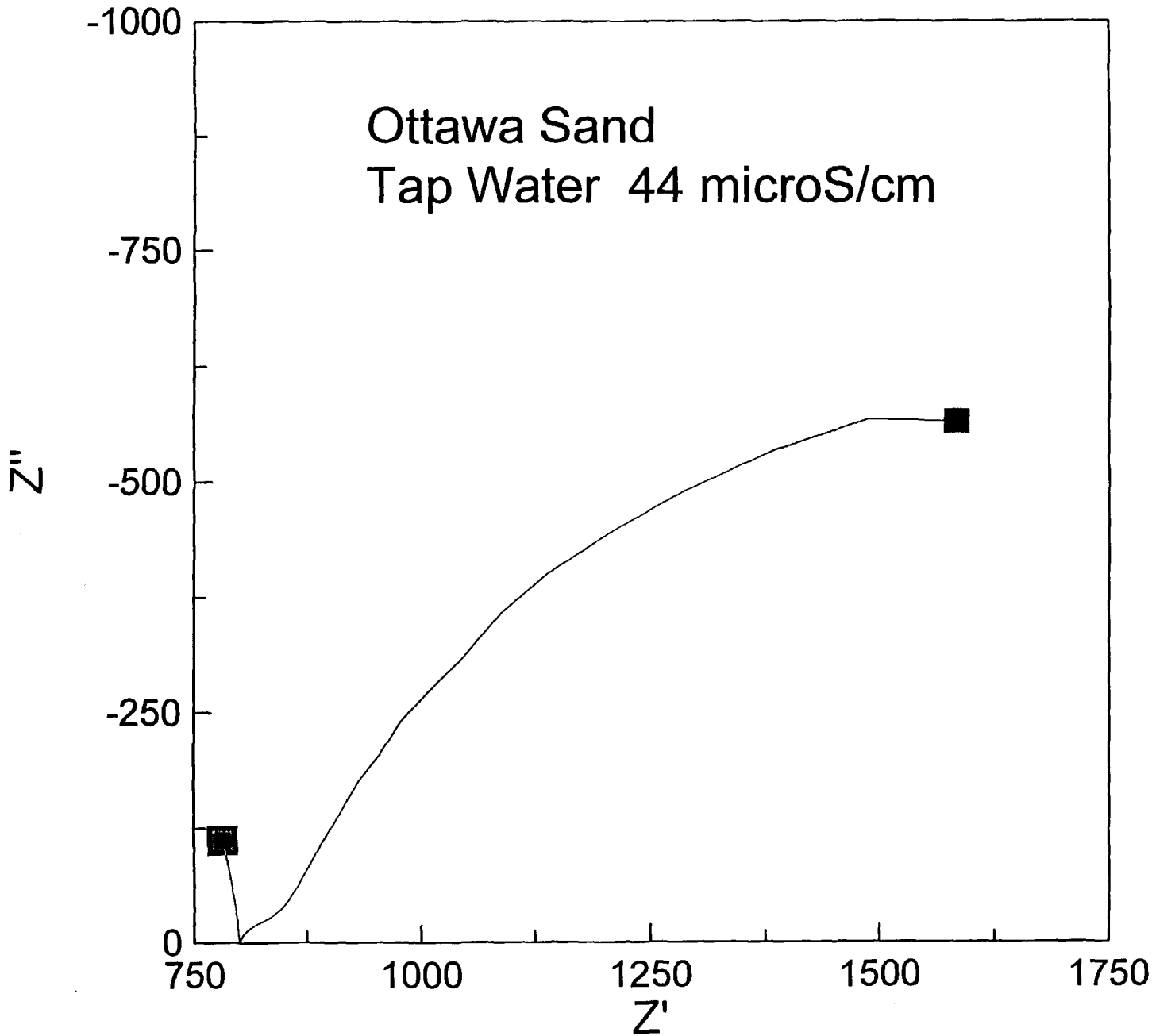
Ottawa Sand
Tap Water 44 microS/cm
-1000
-750
-500
-250
0
Z''
750
1000
1250
1500
1750
Z'

Fig. 6

Figure 6. These are the same data as in Figure 5, plotted slightly differently. Figure 6 is the familiar -Imag. Z vs. Real Z (impedance). Compare also to Figure 7.

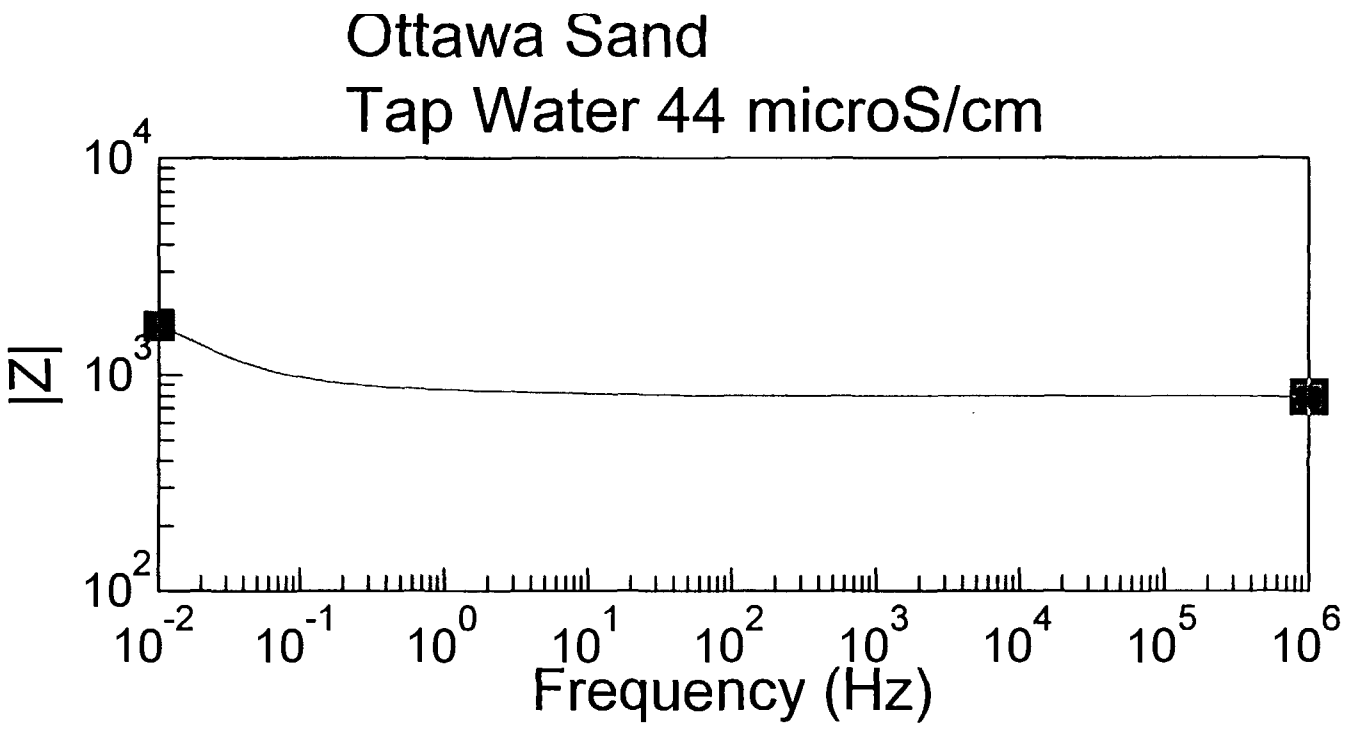
Ottawa Sand
Tap Water 44 microS/cm
|Z|
10^4
10^3
10^2
10^{-2} 10^{-1} 10^0 10^1 10^2 10^3 10^4 10^5 10^6
Frequency (Hz)

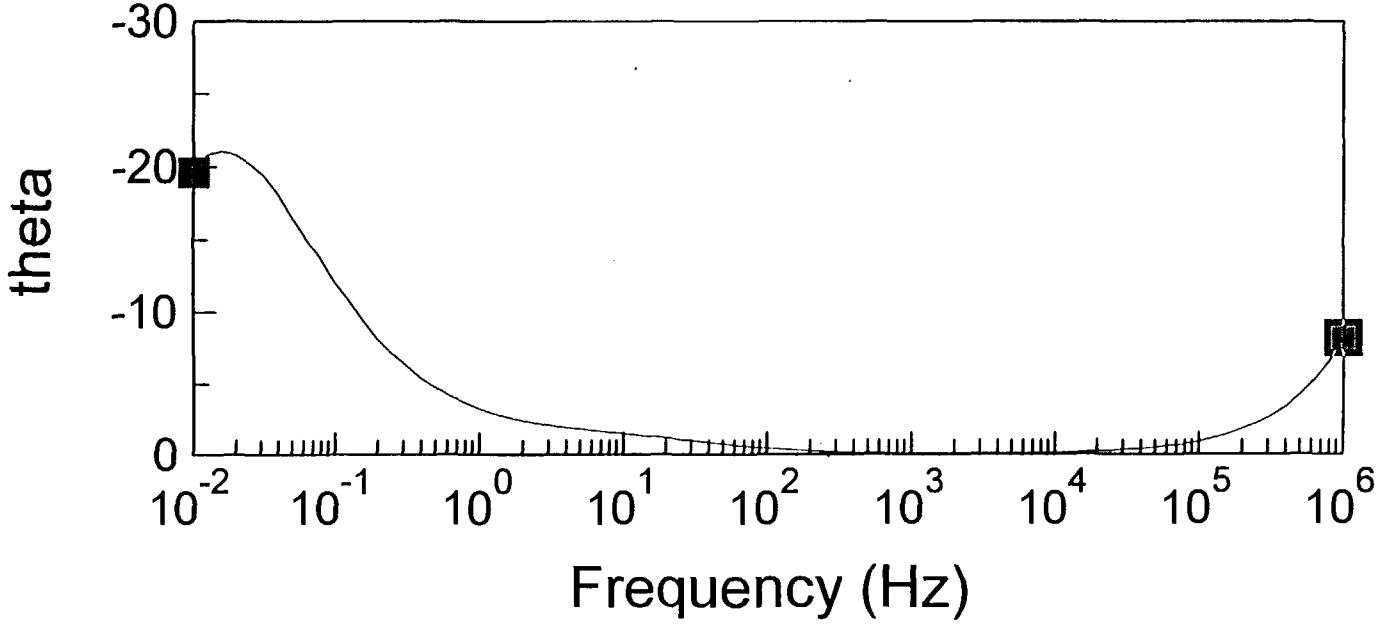
theta
-30
-20
-10
0
10^{-2} 10^{-1} 10^0 10^1 10^2 10^3 10^4 10^5 10^6
Frequency (Hz)

F.g. 7

Figures 7. These are the same data as in Figures 5 and 6, plotted slightly differently. Figure 7 shows impedance magnitude and phase as a function of frequency.

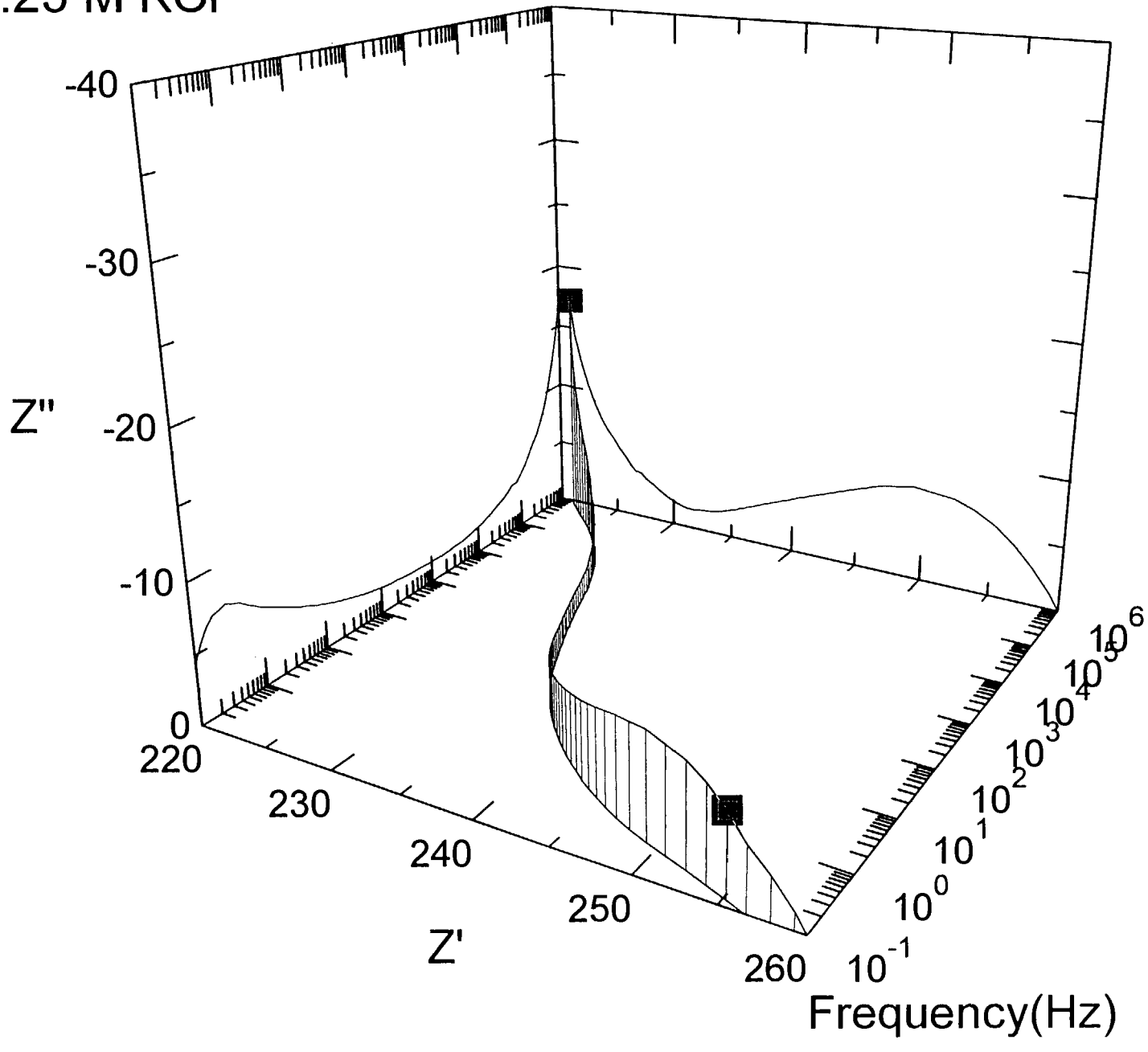
Sample sccsp5
0.25 M KCl
-40
-30
-20
-10
0
Z''
220
230
240
250
260
Z'
10^{-1}
10^{0}
10^{1}
10^{2}
10^{3}
10^{4}
10^{5}
10^{6}
Frequency(Hz)

Fig. 8

Figure 8. This figure shows the frequency dependence of a sample with clay layers in parallel (electrically). It was saturated with 0.25 M KC1 solution (28.6 mS/cm conductivity). This can be contrasted with the response in Figures 5 and 6.

Elastic Wave Velocities

We have measured both compressional- and shear-wave velocities for various sand-clay mixtures and pure sand samples, at ambient pressure conditions as well as using small (about 1 to 15 psi) known axial loads on the samples. We are in the process of reducing and analyzing these data.

In general, we find that our measured velocities are similar to values found in the literature, where available. For example, we find velocities of about 500 m/s for compressional waves in Ottawa sand at low pressures. Our database (see appendix) includes values of about 400 m/s to 600 m/s for similar sand under similar conditions (Rao, 1966), and values of about 300 m/s to 400 m/s for similar sand at pressures of 2, 5, and 25 psi (Whitman, 1966). Consolidated sandstones and unconsolidated sands at higher pressures (e.g., 1500 psi) have much higher velocities, near 1500 m/s (Wyllie et al., 1956; Domenico, 1976). We measured shear wave velocities near 300 m/s in our dry sand sample, at low axial pressure (near 2 psi). We did not find any low-pressure measurements of shear velocities for unconsolidated sediments on land in the literature, but marine sediments are known to have similar shear velocities (e.g., Berge et al., 1991).

Our preliminary results indicate that microstructure controls the velocities, and that clay microstructure is particularly important. We are investigating the effects of flocculation and de-flocculation on mechanical properties, and have submitted an abstract on this topic for presentation at the 1997 Fall Annual Meeting of the American Geophysical Union (Bonner et al., 1997). This abstract is included below, after Figure 9 and Figure 10.

Figure 9 shows an example of one of the samples used for separate elastic wave velocity and electrical properties measurements. (We have since redesigned sample holders for velocity measurements to improve signal quality, and are no longer using the same sample for both sets of measurements.) Figure 10 shows a photograph of the apparatus used to measure compressional- and shear-wave velocities.

Fig. 9

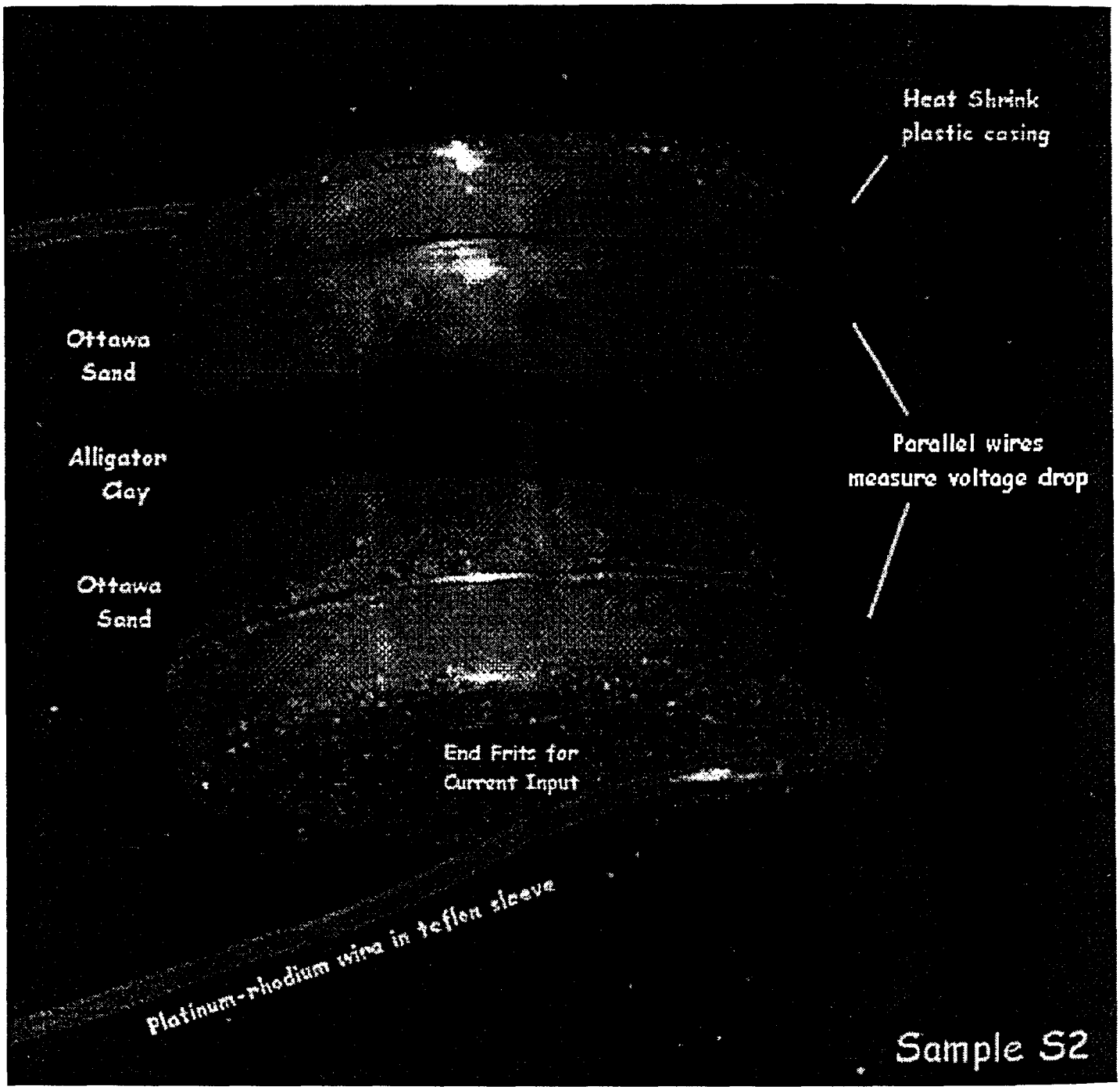
Heat Shrink
plastic casing
Ottawa
Sand
Alligator
Clay
Ottawa
Sand
Parallel wires
measure voltage drop
End Frits for
Current Input
Platinum-rhodium wires in teflon sleeve
Sample S2

Figure 9. Sample design showing construction. The double-layered plastic casing is rigid enough to hold the sample intact and protect its structure, but not rigid enough to affect elastic wave velocity measurements. The sample shown is primarily made up of Ottawa sand with an approximately 1 cm layer of Alligator clay in the center. The transparent casing allows researchers to monitor the condition of the sample to insure that the electrode wires remain parallel, and the internal structure does not change. (This sample design was later changed to improve elastic wave velocity measurement results.)

Fig. 10

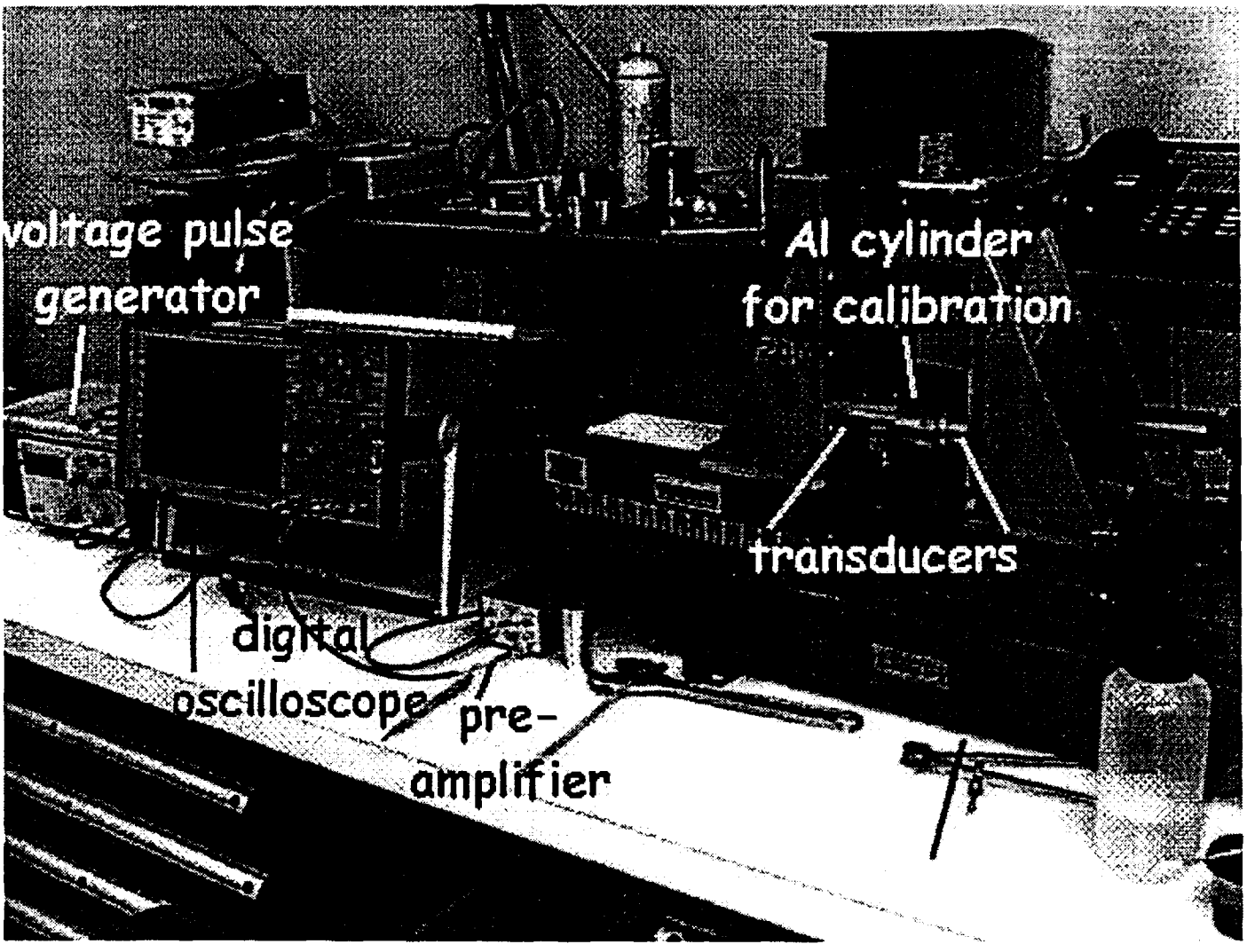
voltage pulse generator
Al cylinder for calibration
transducers
digital oscilloscope
pre-amplifier

Figure 10. Photograph showing experimental setup for elastic wave velocity measurements. Aluminum and steel cylinders of varying lengths and diameters were used to calibrate the apparatus, and find the travel time through the transducer assembly. Various sets of transducers are used.

Abstract from Influence of Chemistry on Physical Properties: Ultrasonic Velocities in Mixtures of Sand and Swelling Clay

B. P. Bonner, D. J. Hart, P. A. Berge, and C. Ruddle
(submitted to 1997 Fall Meeting of the American Geophysical Union)
UCRL-JC-128306abs

Chemistry can significantly influence the physical properties of rocks and sediments. Such effects are particularly important for unconsolidated materials and low pressures, the conditions typical for environmental applications such as imaging the shallow subsurface. It is well known that clay affects sound speeds in sand clay mixtures, for nonswelling clays. These effects can be explained as the physical influence of microstructural changes, and can be modeled with appropriate effective medium theories for estimating physical properties of composites using physical properties of component sands and clays. However, many soil properties such as ultrasonic velocities have not previously been studied systematically. Influential factors include pore fluid chemistry, amount of saturation, degree of consolidation, amount of clay, and related surface effects. The process we focus on is swelling of clays caused by changes in pore fluid composition. We have constructed unconsolidated samples using mixtures of Ottawa sand and Wyoming bentonite, and pore fluids include deionized water and brines of various compositions. We continuously monitor ultrasonic velocities as pore fluid composition is changed, to understand how changes in microstructure induced by chemistry will affect elastic properties.

Progress on Theories

In the past year, three papers on theoretical methods for estimating properties of porous media have been completed (Berryman and Pride, 1997; Dvorkin et al., 1997; Pride and Berryman, 1997). The abstracts from these papers are given below.

Abstract from Volume Averaging, Effective Stress Rules, and Inversion for Microstructural Response of Multicomponent Porous Media

J. G. Berryman and S. R. Pride
(International Journal of Solids and Structures, in press, 1997)
UCRL-JC-127248

A general volume-averaging technique is used to derive equations satisfied by the average scalar stresses and strains in multicomponent porous rock. The resulting equations are combined with general thought experiments to produce the effective-stress rules that determine the volumetric changes of the rock induced by changes in the confining and fluid pressures. The composite porous material specifically treated is an isotropic mixture of two Gassmann materials. Two distinct cases are considered depending on whether the grains at the interface between the Gassmann materials are either 1) welded together (no "cracks" can open between the two constituents) or 2) nonwelded (cracks can open). The effective-stress laws determine not only the overall volumetric changes of a given sample (i.e., changes in sample volume, total pore volume, and fluid-mass content), but determine as well the changes within each Gassmann component individually. This additional level of detail achieved in the analysis is referred to as the inversion for the microstructural response. In the nonwelded case, the effective-stress law relating the variation of crack porosity with macroscopic changes in confining and fluid stress can be used to determine optimum strategies for increasing fracture/crack porosity with applications to reservoir production analysis.

Abstract from Effective Moduli of Particulates with Elastic Cement

J. Dvorkin, M. Le Ravalec, J. Berryman, and A. Nur
(submitted to Mechanics of Materials, 1997)

We give an approximate method for calculating the effective elastic moduli of a close random pack of identical elastic spheres whose pore space is partially or completely filled with elastic cement. To construct the solution we start with the uncemented pack and add small amounts of cement uniformly at every grain contact. The effective moduli of such an aggregate depend on those of the grains and cement (which are, generally, different), and on the amount of cement. Moduli for grain/cement mixtures are available from the contact cementation theory. Next we introduce an isotropic elastic body with void inclusions (e.g., spherical) whose porosity is the same as the porosity of the pack with contact cement. The moduli of the matrix are as yet unknown. We find them by assuming that the effective moduli of the elastic body with inclusions are equal to those of the pack with contact cement. Then an appropriate effective medium theory (e.g., self-consistent or differential effective medium approximation) provides two equations for the bulk and shear moduli of the matrix. Finally, we use the chosen effective medium theory to calculate the moduli of the elastic body with the matrix thus defined whose inclusions are now filled with the cement. We assume that these are also the moduli of the pack whose pore space is completely filled with the cement. To calculate the elastic moduli of the pack whose pore space is partially filled with the cement, we assume that they are those of the elastic body with the matrix thus defined and with two types of inclusions - void and filled with cement. The porosities of this body and of the cemented pack are the same. This result gives one solution to a general and previously unresolved effective medium problem of contacting elastic inclusions embedded in an elastic matrix. It provides a transition from high-porosity cemented to completely cement-filled granular materials. The solution accurately predicts the compressional elastic modulus (the product of the bulk density and P-wave velocity squared) from wave-propagation experiments on cemented glass beads and natural rocks.

Abstract from Connecting Theory to Experiment in Poroelasticity

S. R. Pride and J. G. Berryman

(International Journal of the Mechanics and Physics of Solids, in press, 1997)

The variables controlled and measured in elastostatic laboratory experiments (the volume changes, shape changes, and confining pressures) are ex-

actly related to the appropriate variables of poroelastic field theory (the gradients of the volume-averaged displacement fields and the volume-averaged stresses). The relations between the laboratory and volume-averaged strain measures require the introduction of a new porous-material geometrical term. In the anisotropic case, this term is a tensor that is related both to the presence of porosity gradients and to a type of weighted surface porosity. In the isotropic case, the term reduces to a scalar and depends only on the surface-porosity parameter. When this surface-porosity parameter is identical to the usual volume porosity, the relations initially proposed by Biot and Willis are recovered. The exact statement of the poroelastic strain-energy density is derived and is used to relate the moduli measured in laboratory experiments to the moduli of poroelastic theory. Only two restrictions are placed on the materials being treated: 1) the fluid is homogeneous in each sample and 2) the material possesses a rigidity. However, the entire work is limited to linear deformations and long (relative to sample size) wavelengths of applied stress.

Summary

This report summarizes progress made on laboratory measurements of elastic wave velocities and electrical properties in sand-clay mixtures, creation of a database containing elastic velocity data for unconsolidated sediments from the engineering and earth science literature, and recent rock physics theory advancements. We are continuing to analyze the laboratory measurements. Next we will make similar measurements on natural soils containing known contaminants. We are using the database and theories to develop algorithms to link geophysical parameters to porosity and saturation, for use in the inversion code. The next step will be to test the algorithms on data for the LLNL contaminated site. When we have finished analyzing our laboratory results, we will submit them to a peer-reviewed journal for publication. Progress made in the first year of this three-year project has built a solid foundation for progress in the second year.

Acknowledgments

This work was performed under the auspices of the U. S. Department of Energy by the Lawrence Livermore National Laboratory under contract No. W-7405-ENG-48 and supported specifically by the DOE Office of Energy Research within the Office of Basic Energy Sciences, Division of Engineering and Geosciences. This project is funded as part of the Environmental Management Science Program (EMSP), a pilot program managed jointly by

the Office of Energy Research and the Office of Environmental Management.

References

Archie, G. E., 1942, The electrical resistivity log as an aid in determining some reservoir characteristics: *Trans. AIME,* **146,** 54-62.

Berge, P. A., S. Mallick, G. J. Fryer, N. Barstow, J. A. Carter, G. H. Sutton, and J. I. Ewing, 1991, *In situ* measurement of transverse isotropy in shallow-water marine sediments: *Geophys. J. Int.,* **104,** 241-254.

Berge, P. A., G. J. Fryer, and R. H. Wilkens, 1992, Velocity-porosity relationships in the upper oceanic crust: Theoretical considerations: *J. Geophys. Res.,* **97,** 15239-15254.

Berge, P. A., J. G. Berryman, and B. P. Bonner, 1993, Influence of microstructure on rock elastic properties: *Geophys. Res. Lett.,* **20,** 2619-2622.

Berge, P. A., B. P. Bonner, and J. G. Berryman, 1995, Ultrasonic velocity-porosity relationships for sandstone analogs made from fused glass beads: *Geophysics,* **60,** 108-119.

Berryman, J. G., 1995, Mixture theories for rock properties, *in* Ahrens, T. J., Ed., *Rock Physics and Phase Relations, A Handbook of Physical Constants,* Am. Geophys. Union, Washington, D.C., 205-228.

Berryman, J. G., and P. A. Berge, 1996, Critique of two explicit schemes for estimating elastic properties of multiphase composites: *Mechanics of Materials,* **22,** *149-164.*

Berryman, J. G., and S. R. Pride, 1997, Volume averaging, effective stress rules, and inversion for microstructural response of multicomponent porous media: *ht. J. Sol. Struct.,* in press.

Bonner, B. P., D. J. Hart, P. A. Berge, and C. Ruddle, 1997, Influence of chemistry on physical properties: Ultrasonic velocities in mixtures of sand and swelling clay: submitted to the *Fail Meeting of the American Geophysical Union.*

Cheng, C. H., 1978, Seismic velocities in porous rocks: direct and inverse problems: *Ph.D. thesis,* Mass. Inst. of Technol., Cambridge, Mass.

Domenico, S. N., 1976, Effect of brine-gas mixture on velocity in an unconsolidated sand reservoir: *Geophysics,* **41,** 882-894.

Dvorkin, J., M. Le Ravalec, J. Berryman, and A. Nur, 1997, Effective moduli of particulates with elastic cement: submitted to *Mechanics of Materials.*

Garrouch, A. A., and M. M. Sharma, 1994, The influence of clay content, salinity, stress, and wettability on the dielectric properties of brine-saturated

rocks: 10 Hz to 10 MHz: *Geophysics,* **59,** 909-917.

Harris, J. M., 1988, High frequency cross-well seismic measurements in sedimentary rocks: *58th Annual Internat. Mtg., Soc. Expl. Geophys., Expanded Abstracts, 147-150.*

Harris, J. M., R. C. Nolen-Hoeksema, R. T. Langan, M. Van Schaack, S. K. Lazaratos, and J. W. Rector III, 1995, High-resolution crosswell imaging of a west Texas carbonate reservoir: Part l-Project summary and interpretation: *Geophysics,* **60,** 667-681.

Lines, L. R., M. Miller, H. Tan, R. Chambers, and S. Treitel, 1993, Integrated interpretation of borehole and crosswell data from a west Texas field: *The Leading Edge,* **12,** 13-16.

Mathisen, M. E., A. A. Vassiliou, P. S. Cunningham, J. Shaw, J. H. Justice, and N. J. Guinzy, 1995, Time-lapse crosswell seismic tomogram interpretation: Implications for heavy oil reservoir characterization, thermal recovery process monitoring, and tomographic imaging technology: Geo*physics,* **60,** 631-650.

Olhoeft, G. R., 1985, Low-frequency electrical properties: *Geophysics,* **50,** *2492-2503.*

Olhoeft, G. R., and T. V. V. King, 1991, Mapping subsurface organic compounds noninvasively by their reactions with clays: *Proc. of the 4th Toxic Substances Hydrology Tech. Mtg., USGS, 552-557.*

Pride, S. R., and J. G. Berryman, 1997, Connecting theory to experiment in poroelasticity: *J. Mech. Phys. Sol.,* in press.

Ramirez, A., W. Daily, D. LaBrecque, E. Owen, and D. Chesnut, 1993, Monitoring an underground steam injection process using electrical resistance tomography: *Water Resources Res.,* **29,** *73-87.*

Ramirez, A. L., W. D. Daily, and R. L. Newmark, 1995, Electrical resistance tomography for steam injection monitoring and process control: *J. Env. Eng. Geophys.,* **0,** *39-51.*

Rae, H. A. B., 1966, Wave velocities through partially saturated sand-clay mixtures: *Massachusetts Institute of Technology Dept. of Civil Engineering Research Report,* R66-13.

Waxman, M. H., and J. M. Smits, 1968, Electrical conductivities in oil-bearing shaly sands: Soc. *Pet. Eng. J., Trans. AIME,* **243,** *107-222.*

Whitman, R. V., 1966, Miscellaneous studies of the formation of wave fronts in sand: *Massachusetts Institute of Technology Dept. of Civil Engineering Research Report,* R66-32.

Wilt, M., II. F. Morrison, A. Becker, H.-W. Tseng, K. Lee, C. Torres-Verdin, and D. Alumbaugh, 1995a, Crosshole electromagnetic tomography: A new technology for oil field characterization: *The Leading Edge,* **14,** 173-177.

Wilt, M. J., D. L. Alumbaugh, H. F. Morrison, A. Becker, K. H. Lee, and M. Deszcz-Pan, 1995b, Crosswell electromagnetic tomography: System design considerations and field results: *Geophysics,* **60,** 871-885.

Wyllie, M. R. J., A. R. Gregory, and L. W. Gardner, 1956, Elastic wave velocities in heterogeneous and porous media: *Geophysics,* **21,** 41-70.

Wyllie, M. R. J., A. R. Gregory, and G. H. F. Gardner, 1958, An experimental investigation of factors affecting elastic wave velocities in porous media: *Geophysics,* **23,** 459-493.

Appendix

Elastic Properties of Unconsolidated Sediments at Low Pressures

(examples from the marine geophysics, civil engineering, soil mechanics, exploration geophysics, and environmental geophysics literature)

Data Source	Sample Type	State of Consolidation	Density (g/cm3)	Vp (km/s)
Hamilton, *Geoacoustic modeling of the sea floor, 1980*	course sand	U	2.034	1.836
	fine sand	U	1.941	1.749
	very fine sand	U	1.856	1.702
	silty sand	U	1.772	1.646
	sandy silt	U	1.771	1.652
	silt	U	1.740	1.615
	sand-silt-clay	U	1.596	1.579
	clayey silt	U	1.488	1.549
	silty clay	U	1.421	1.520
Hamilton and Bachman, Sound velocity and related properties of marine sediments, 1982	course sand	U	2.034	1.836
	fine sand	U	1.962	1.759
	very fine sand	U	1.878	1.709
	silty sand	U	1.783	1.658
	sandy silt	U	1.769	1.644
	silt	U	1.740	1.615
	sand-silt-clay	U	1.575	1.582
	clayey silt	U	1.489	1.546
	silty clay	U	1.480	1.517
Bourbie, Coussy & Zinszner, Acoustics of porous media, 1987	clean sandstone	C		
	sandstone	C		
	chalk	C		
	fine limestone	C		
	oolitic limestone	C		
	bioclastic limestone	C		
	sintered glass beads 1	C		4.050
	sintered glass beads 2	C		4.840
	sintered glass beads 3	C		5.150
	3 M-55	C		2.760
	3 M-40	C		2.910
	Coors			3.950
	Porous steel			2.740
	Porous titanium			2.720
	Porous Inconel			2.120
	Filtros #1			4.650

Chan, Newmark, Mavko and Beuttner, Conductivity of sand-clay mixtures	1% kaolinite and 99% ottawa sand (01KOT-1)	U		1.810
	1% kaolinite and 99% ottawa sand (01KOT-2)	U		0.610
	5% kaolinite and 95% ottawa sand (05KOT-1)	U		no data
	5% kaolinite and 95% ottawa sand (05KOT-2)	U		0.780
	10% kaolinite and 90% ottawa sand (10KOT-1)	U		0.840
	10% kaolinite and 90% ottawa sand (10KOT-3)	U		1.870
	10% kaolinite and 90% ottawa sand (10Clay-1)	U		not taken
	25% kaolinite and 75% ottawa sand (25Clay-1)	U		not taken
	25% kaolinite and 75% ottawa sand (25KOT-2)	U		1.910
	50% kaolinite and 50% ottawa sand (50KOT-2)	U		1.050
	100% ottawa sand (OT-1)	U		2.240
	100% oklahoma sand (OK-1)	U		not taken
	Glass beads (GB-1)			not taken
	Glass beads (GL-1)			2.290
	Alligator Clay (ALL-1)	U		not taken
	Crot Sandy loam (CROT-1)	U		not taken
	Water Experiment Station Soil (WES-1)	U		not taken
	CalTrans soil (BU-1)	U		2.030
	Jane's soil (JA-1)	U		2.370
	Craig's soil (CR-1)	U		2.220

Green, Wang and Bonner, *Shear wave attenuation in dry and saturated sandstone at seismic to ultrasonic frequencies,* 1993	Berea sandstone	C		
	Berea sandstone	C		
	Berea sandstone	C		
	Berea sandstone	C		
	Berea sandstone	C		
	Berea sandstone	C		
	Berea sandstone	C		
	Berea sandstone	C		
	Berea sandstone	C		
	Berea sandstone	C		
	Berea sandstone	C		
	Berea sandstone	C		
	Berea sandstone	C		
	Fused glass beads	C		
	fused glass beads	C		
	fused glass beads	C		
Fatt, *Compressibility of sandstones at low to moderate pressures,* 1958	Feldspathic graywacke, Brea Canyon	C		
	Felspathic graywacke, Huntington beach	C		
	Feldspathic graywacke, West Montalvo	C		
	Arkose, West Montalvo	C		
	Lithic Graywacke, Oxnard	C		
	Feldspathic graywacke, Oxnard	C		
	graywacke, Oxnard	C		
	Arkose, Ventura	C		
	Arkose, San Joaquin Valley	C		
	Feldspathic graywacke, San Joaquin Valley	C		
	Feldspathic graywacke, San Joaquin Valley	C		
	Lithic graywacke, San Joaquin Valley	C		

	Arenaceous Limestone, San Joaquin Valley	C		
	Subgraywacke, Bradford, PA	C		
	Felspathic Quartzite, Sherman, TX	C		
	Feldspatic graywacke, Kelly-Snyder, TX	C		
	subgraywacke, Kelly-Snyder, TX	C		
	Feldspatic Quartzite, Colo	C		
	Subarkose, Colo	C		
	Feldspatic Quartzite, Wyoming	C		
	Orthoquartzite, Wyoming	C		
	Orthoquartzite, Nevada	C		
	Arkose, Louisiana	C		
	Feldspathic graywacke, Louisiana	C		
	Feldspathic graywacke, South Ward, TX	C		
	Unconsolidated sand	U		
	Sintered aluminum oxide	C		
Wyllie, Gregory and Gardner, *Elastic Wave Velocities in heterogeneous and porous media,* 1956	Cromwell sandstone	C		2.515
	Cromwell sandstone	C		2.896
	Cromwell sandstone	C		2.835
	Cromwell sandstone	C		2.927
	Cromwell sandstone	C		2.896
	Cromwell sandstone	C		3.115
	Cromwell sandstone	C		3.110
	Cromwell sandstone	C		3.231
	Nichols Buff sandstone	C		1.677
	Nichols Buff sandstone	C		1.723
	Nichols Buff sandstone	C		1.753
	Nichols Buff sandstone	C		1.829
	Nichols Buff sandstone	C		1.890
	Nichols Buff sandstone	C		2.348
	Nichols Buff sandstone	C		2.287

	Nichols Buff sandstone	C		2.561
	Britton, Okla. sandstone	C		1.829
	Britton, Okla. sandstone	C		1.723
	Britton, Okla. sandstone	C		1.601
	Britton, Okla. sandstone	C		1.646
	Britton, Okla. sandstone	C		1.631
	Britton, Okla. sandstone	C		1.768
	Britton, Okla. sandstone	C		1.692
	Britton, Okla. sandstone	C		2.241
glass velocity= 5.486	glass spheres saturated with brine		1.14	1.707
plastic velocity= 2.651	glass spheres saturated with water		1.00	1.469
glass density = 2.4g/cc	saturated with C2H5OH		0.79	1.158
plastic density = 1.17g/cc	glass spheres saturated with CCl4		1.50	0.914
	glass spheres saturated with oil		0.75	1.216
	glass spheres saturated with Silicone		0.76	0.875
	glass spheres saturated with air		0.00	0.344
	plastic spheres saturated with water		1.00	1.469
Wyllie, Gregory and Gardner, *An Experimental Investigation of Factors Affecting Elastic Wave Velocities in Porous Media,* 1958	Berea Sandstone	C		9.700
	Berea Sandstone	C		11.100
	Berea Sandstone	C		11.400
	Berea Sandstone	C		11.700
	Berea Sandstone	C		12.000
	Berea Sandstone	C		12.300
	Berea Sandstone	C		12.500

	Berea Sandstone	C		12.550
	Berea Sandstone	C		12.600
	Berea Sandstone	C		12.650
	Berea Sandstone	C		12.650
	Berea Sandstone	C		12.650
Domenico, *Effect of brine-gas mixture on velocity in an unconsolidated sand reservoir,* 1976	Ottawa sand, saturated with brine	U		1.255
	Ottawa sand, saturated with brine	U		1.255
	Ottawa sand, saturated with brine	U		1.266
	Ottawa sand, saturated with brine	U		1.260
	Ottawa sand, saturated with brine	U		1.294
	Ottawa sand, saturated with brine	U		2.030
	Ottawa sand, saturated with brine	U		2.060
	Ottawa sand, saturated with brine	U		2.072
	Glass bead speciman			2.090
	Glass bead speciman			1.102
Rao, *Wave velocities through partially saturated sand-clay mixtures,* 1966	Dispersed kaolinite	U		
	Dispersed kaolinite	U		
	dispersed Boston blue clay	U		
	dispersed Boston blue clay	U		
	dispersed Boston blue clay	U		
	dispersed Boston blue clay	U		
	flocculated Boston blue clay	U		
	flocculated Boston blue clay	U		
	flocculated Boston blue clay	U		

	flocculated Boston blue clay	U		
	flocculated Boston blue clay	U		
	flocculated Boston blue clay	U		
	flocculated Boston blue clay	U		
	tap water kaolinite	U		
	tap water kaolinite	U		
	tap water kaolinite	U		
	tap water kaolinite	U		
	tap water kaolinite	U		
	salt flocculated kaolinite	U		
	salt flocculated kaolinite	U		
	salt flocculated kaolinite	U		
	salt flocculated kaolinite	U		
	salt flocculated kaolinite	U		
	salt flocculated kaolinite	U		
	salt flocculated kaolinite	U		
	salt flocculated kaolinite	U		
	salt flocculated kaolinite	U		
	salt flocculated kaolinite	U		
	salt flocculated kaolinite	U		
	salt flocculated kaolinite	U		
	salt flocculated kaolinite	U		

Nur and Vernik, *Petrophysical Classification of Siliciclastics for Lithology and Porosity Prediction from Seismic Velocities,* 1992	Quartz-kaolinite mixture, 0% clay	U		
	Quartz-kaolinite mixture, 10% clay	U		
	Quartz-kaolinite mixture, 20% clay	U		
	Quartz-kaolinite mixture, 30% clay	U		
	Quartz-kaolinite mixture, 37% clay	U		
	Quartz-kaolinite mixture, 49% clay	U		
	Quartz-kaolinite mixture, 59% clay	U		
Blangy, Strandenes, Moos and Nur, *Ultrasonic velocities in sands-revisited,* 1991	Troll Sands (loosely consolidated subarkosic sands with little clay)	U		3.200
	Troll Sands	U		2.700
	Troll Sands	U		2.500
Marion, Nur, Yin and Han, *Compressional velocity and porosity in sand-clay mixtures,* 1989	Ottawa sand	U		2.149
	Ottawa sand	U		2.280
	Ottawa sand	U		2.415
	Ottawa sand	U		2.485
	Ottawa sand	U		2.540

Vs (km/s)	Velocity Ratio	Porosity %	Permeability (md)	Pressure (MPa)	Saturation %
	1.201	38.6%			
	1.145	45.6%			
	1.115	50.0%			
	1.078	55.3%			
	1.080	54.1%			
	1.057	56.3%			
	1.033	66.3%			
	1.014	71.6%			
	0.994	75.9%			
	1.201	38.6%			
	1.152	44.5%			
	1.120	48.5%			
	1.086	54.2%			
	1.076	54.7%			
	1.057	56.2%			
	1.036	66.3%			
	1.012	71.6%			
	0.990	73.0%			
		11.0%	220		
		22.0%	1700		
		42.0%	2.4		
		28.0%	25		
		15.0%	80		
		34.0%	1100		
2.37		28.3%			
2.93		18.5%			
2.97		10.5%			
1.41		34.5%			
1.62		30.0%			
2.16		41.5%			
1.54		48.0%			
1.79		41.0%			
1.15		36.0%			
2.91		40.0%			

		33.4%			
		37.7%			
		33.4%			
		37.0%			
		32.6%			
		33.1%			
		38.0%			
		46.0%			
		32.9%			
		35.1%			
		34.2%			
		40.0%			
		42.0%			
		37.2%			
		50.0%			
		49.9%			
		50.3%			
		31.6%			
		35.3%			
		34.5%			

2.23		18-21%	100	7	
2.32		18-21%	100	10	
2.40		18-21%	100	10	
2.46		18-21%	100	20	
2.55		18-21%	100	30	
2.58		18-21%	100	50	
2.57		18-21%	100	70	
2.31		18-21%	300	20	
2.35		18-21%	300	30	
2.41		18-21%	300	70	
2.32		18-21%	450	60	
2.32		18-21%	450	70	
2.22		31.5%		20	
2.23		31.5%		30	
2.28		31.5%		70	
		18.7%			
		24.0%			
		9.9%			
		15.2%			
		9.0%			
		11.2%			
		10.2%			
		10.7%			
		17.6%			
		21.4%			
		19.9%			
		8.9%			

		23.5%			
		14.5%			
		12.6%			
		16.9%			
		19.2%			
		21.1%			
		11.3%			
		14.4%			
		9.3%			
		9.0%			
		24.1%			
		16.6%			
		11.8%			
		36.0%			
		28.6%			
		16.3%			0.0%
		16.3%			17.0%
		16.3%			45.0%
		16.3%			62.0%
		16.3%			77.0%
		16.3%			89.0%
		16.3%			95.0%
		16.3%			100.0%
		21.7%			0.0%
		21.7%			50.0%
		21.7%			63.0%
		21.7%			72.0%
		21.7%			83.0%
		21.7%			92.0%
		21.7%			96.0%

		21.7%			100.0%
		29.9%			0.0%
		29.9%			5.0%
		29.9%			57.0%
		29.9%			76.0%
		29.9%			83.0%
		29.9%			92.0%
		29.9%			96.0%
		29.9%			100.0%
		20.0%		0	
		20.0%		0.5	
		20.0%		1	
		20.0%		1.7	
		20.0%		3	
		20.0%		3.5	
		20.0%		4.5	

		20.0%		5.7	
		20.0%		6.2	
		20.0%		7.4	
		20.0%		8.7	
		20.0%		10	
0.836					0.0%
0.829					50.4%
0.829					55.6%
0.827					66.7%
0.813					86.5%
0.783					93.9%
0.802					97.4%
0.801					100.0%
0.704					94.6% (flow
0.668					94.9% (imb
0.396		37.5%		0.7	
0.305		41.2%		0.28	
0.427		39.4%		0.7	
0.411		39.4%		0.7	
0.296		41.2%		0.28	
0.283		41.2%		0.28	
0.411		37.5%		0.7	
0.381		37.5%		0.7	
0.366		37.5%		0.7	

0.274		39.4%		0.28	
0.268		39.4%		0.28	
0.305		37.5%		0.28	
0.297		37.5%		0.28	
0.378		47.4%		0.7	
0.351		48.7%		0.7	
0.253		49.2%		0.28	
0.274		51.7%		0.28	
0.244		53.5%		0.28	
0.290		50.0%		0.7	
0.287		50.0%		0.7	
0.302		51.2%		0.7	
0.282		51.9%		0.7	
0.255		51.0%		0.28	
0.244		50.7%		0.28	
0.244		51.0%		0.28	
0.235		51.0%		0.28	
0.235		51.9%		0.28	
0.213		54.5%		0.28	
0.219		55.0%		0.28	
0.213		56.1%		0.28	
0.216		57.1%		0.28	

		33.0%			
		33.0%			
		26.0%			
		18.0%			
		13.0%			
		14.0%			
		16.0%			
1.7		23.0%		30	
1.4		30.0%		30	
1.2		36.5%		30	
0.836				10	
0.932				20	
1.028				30	
1.109				40	
1.156				50	